Protein Science (1999), *8*:1930–1945. Cambridge University Press. Printed in the USA.
Copyright © 1999 The Protein Society

CJ

Allosteric inhibition of glycogen phosphorylase *a* by the potential antidiabetic drug 3-isopropyl 4-(2-chlorophenyl)-1,4-dihydro-1-ethyl-2-methyl-pyridine-3,5,6-tricarboxylate

NIKOS G. OIKONOMAKOS,[1] KATERINA E. TSITSANOU,[1] SPYROS E. ZOGRAPHOS,[1] VICKY T. SKAMNAKI,[1] SIEGFRIED GOLDMANN,[2] AND HILMAR BISCHOFF[2]

[1]Institute of Biological Research and Biotechnology, The National Hellenic Research, 48 Vas. Constantinou Avenue, Athens 11635, Greece

[2]Bayer AG, Geschaftsbereich Pharma Research, Chemische Forschung (SG & AS), and Institute f. Herz-Kreislauf- und-Arteriosklerose-Forschung (HS), D-42096 Wuppertal, Germany

(RECEIVED April 5, 1999; ACCEPTED June 7, 1999)

Abstract

The effect of the potential antidiabetic drug (-)(*S*)-3-isopropyl 4-(2-chlorophenyl)-1,4-dihydro-1-ethyl-2-methyl-pyridine-3,5,6-tricarboxylate (W1807) on the catalytic and structural properties of glycogen phosphorylase *a* has been studied. Glycogen phosphorylase (GP) is an allosteric enzyme whose activity is primarily controlled by reversible phosphorylation of Ser14 of the dephosphorylated enzyme (GPb, less active, predominantly T-state) to form the phosphorylated enzyme (GPa, more active, predominantly R-state). Upon conversion of GPb to GPa, the N-terminal tail (residues 5–22), which carries the Ser14(P), changes its conformation into a distorted 3_{10} helix and its contacts from intrasubunit to intersubunit. This alteration causes a series of tertiary and quaternary conformational changes that lead to activation of the enzyme through opening access to the catalytic site. As part of a screening process to identify compounds that might contribute to the regulation of glycogen metabolism in the noninsulin dependent diabetes diseased state, W1807 has been found as the most potent inhibitor of GPb (K_i = 1.6 nM) that binds at the allosteric site of T-state GPb and produces further conformational changes, characteristic of a T′-like state. Kinetics show W1807 is a potent competitive inhibitor of GPa (-AMP) (K_i = 10.8 nM) and of GPa (+1 mM AMP) (K_i = 19.4 μM) with respect to glucose 1-phosphate and acts in synergism with glucose. To elucidate the structural features that contribute to the binding, the structures of GPa in the T-state conformation in complex with glucose and in complex with both glucose and W1807 have been determined at 100 K to 2.0 Å and 2.1 Å resolution, and refined to crystallographic *R*-values of 0.179 (R_{free} = 0.230) and 0.189 (R_{free} = 0.263), respectively. W1807 binds tightly at the allosteric site and induces substantial conformational changes both in the vicinity of the allosteric site and the subunit interface. A disordering of the N-terminal tail occurs, while the loop of chain containing residues 192–196 and residues 43′-49′ shift to accommodate the ligand. Structural comparisons show that the T-state GPa-glucose-W1807 structure is overall more similar to the T-state GPb-W1807 complex structure than to the GPa-glucose complex structure, indicating that W1807 is able to transform GPa to the T′-like state already observed with GPb. The structures provide a rational for the potency of the inhibitor and explain GPa allosteric inhibition of activity upon W1807 binding.

Keywords: allosteric site; crystal structure; diabetes; glycogen metabolism; inhibition; phosphorylase *a*

BEST AVAILABLE COPY

Reprint requests to: Dr. N.G. Oikonomakos, Institute of Biological Research and Biotechnology, The National Hellenic Research, 48 Vas. Constantinou Avenue, Athens 11635, Greece; e-mail: nikos@aegean.eie.gr.

Abbreviations: GP, glycogen phosphorylase, 1,4-α-D-glucan:orthophosphate α-glucosyltransferase (EC 2.4.1.1); GPb, glycogen phosphorylase *b*; GPa, glycogen phosphorylase *a*; PLP, pyridoxal 5′-phosphate; Glc, α-D-glucose; Glc-1-*P*, α-D-glucose 1-phosphate; W1807, (-)(*S*)-3-isopropyl 4-(2-chlorophenyl)-1,4-dihydro-1-ethyl-2-methyl-pyridine-3,5,6-tricarboxylate; Bes, N,N-bis(2-hydroxy-ethyl)-2-aminomethane sulfonic acid; DTT, dithiothreitol; EDTA, ethylenediaminetetraacetic acid; PDB, Protein Data Bank; RMSD, root-mean-square deviation.

Glycogen phosphorylase (GP), a key-enzyme in the regulation of glycogen metabolism, catalyzes the degradative phosphorolysis of glycogen to glucose 1-phosphate (Glc-1-*P*). In muscle, Glc-1-*P* is utilized via glycolysis to generate metabolic energy, and in the liver it is converted to glucose (Glc). The enzyme exists in two interconvertible forms: the dephosphorylated form, GPb, and the phosphorylated form, GPa. In resting muscle the enzyme exists in the inactive form (GPb), which can be activated either by non-covalent cooperative binding of AMP (or IMP) or by covalent phosphorylation to form GPa. GPa does not require AMP for ac-

tivation, although addition of AMP can produce a 10–20% increase in activity. Both forms can exist in a less active T-state and a more active R-state according to the Monod–Wyman–Changeux model for allosteric proteins (Monod et al., 1965). The T-state is stabilized by the binding of ATP, Glc-6-*P*, Glc, and caffeine, and the R-state is induced by AMP (or IMP) substrates or certain substrate analogues (Johnson et al., 1989; Johnson, 1992; Oikonomakos et al., 1992). GPa has escaped some of the allosteric controls to which GPb is subject, because activity is no longer inhibited appreciably by ATP or Glc-6-P. In fact, ATP inhibits that extra activity caused by the AMP (Fletterick & Madsen, 1980), while Glc-6-P inhibits the enzyme at nonphysiological concentrations (Melpidou & Oikonomakos, 1983).

X-ray diffraction studies (Sprang et al., 1988; Barford & Johnson, 1989; Barford et al., 1991; Sprang et al., 1991) have shown the conformational changes that take place following activation of the muscle enzyme on conversion from the T- to R-state by phosphorylation or AMP. In the T-state structure of GPb, N-terminal residues 10–22 (residues 1–10 are not located) are in an extended β-stranded conformation, are poorly ordered, and make intrasubunit contacts. On phosphorylation, there is a dramatic conformational change so that the N-terminal residues, 10 to 22, swing through 120° with respect to their position in GPb and change their structure to a distorted 3_{10} helix and their contacts to intersubunit (Fig. 1). The Ser14-*P* forms ion pairs with Arg69 of the α2 helix (residues 47–78) and Arg43′ in the cap′ (residues 36′ to 47′) of the symmetry-related subunit. On activation by AMP, a high affinity AMP binding site is formed, which involves residues Asp42′, Asn44′, and Val45′ from the cap′, residues Gln71 and Tyr75 from the α2 helix, residues Arg309 and Arg310 from the α8 helix (residues 289–314), and residues from the 315–325 loop (the loop following helix α8), which is ordered and appears to be an important AMP binding determinant. Furthermore, in the PLPP-GP*b*-AMP (Sprang et al., 1991) complex structure, the N-terminal residues were found to be partially ordered in a similar conformation to that observed in GPa with the exception that the crucial side chains of Arg43′ and Arg69 are not located. The signals from either phosphorylation or AMP activation are transmitted via the quaternary structural changes and extensive changes in tertiary structure at the subunit interface. On the T to R transition, the quaternary structural change is represented by a rotation of each subunit by 5° about an axis positioned close to the cap′/α2 interface. As a result, the cap′/α2 interface is tightened and the other major interface comprising the tower helices (residues 262 to 276) is weakened, allowing communication of events at the allosteric site to those at the catalytic site and vice versa (Barford & Johnson, 1989). Residues from the top of the tower are in van der Waals' contact with side chains in the 280s loop of the other subunit, and this indirect connection between the catalytic site and the subunit interface is of key importance for the transmission of conformational changes from one subunit to the other. On transition from T- to R-state, the 280s loop becomes disordered and displaced, thus opening a channel that allows substrate access to the catalytic site. The catalytic site is buried approximately 15 Å from the surface and is close to the cofactor pyridoxal phosphate (Fig. 1). Glc (or Glc analogues) bind at the catalytic site and promote the T-state, through stabilization of the closed position of the 280s loop. Caffeine can bind simultaneously, at the inhibitor site, situated at the entrance to the catalytic site (some 10 Å from it) and inhibit enzyme activity synergistically (with Glc).

Glc is a physiological regulator of hepatic glycogen metabolism that promotes inactivation of GPa and acts synergistically with insulin leading to diminished glycogen degradation and enhanced glycogen synthesis (Bollen & Stalmans, 1992). It has been postulated that Glc analogues with greater inhibition of GPa may result in more effective regulatory agents than Glc and that powerful and specific inhibitors of GP should shift the balance between glycogen breakdown and glycogen synthesis in favor of the latter (Martin et al., 1991). Such compounds may be of therapeutic benefit in the treatment of the noninsulin-dependent (Type 2) form of diabetes mellitus.

During the last five years, a systematic work has been carried out involving structure assisted design, synthesis, kinetic characterization, and crystallographic binding studies that led to the dis-

Fig. 1. A schematic diagram of the GPa dimeric molecule viewed down the twofold axis for residues 5 to 838. The positions are shown for the catalytic, allosteric, phosphorylation, and the inhibitor site. The catalytic site, which includes the essential cofactor pyridoxal phosphate (PLP; yellow), is buried at the centre of the subunit accessible to the bulk solvent through a 15 Å long channel. Glc (shown in orange), a competitive inhibitor of the enzyme that also promotes the less active T-state through stabilization of the closed position of the 280s loop (shown in white), binds at this site. The allosteric site, which binds the activator AMP, other phosphorylated compounds such as ATP, and the allosteric inhibitor W1807 (shown in magenta), is situated at the subunit–subunit interface (between the cap′ (of the other subunit), the α2 helix and the α8 helix) some 30 Å from the catalytic site. Residues of the allosteric site(s), interacting with W1807, are shown highlighted in both subunits. The phosphorylation site (Ser14), which, in the T-state GPb, is located close to an acidic site on the surface of the enzyme (residues 13–24 shown in yellow), on activation by phosphorylation adopts a different location at the subunit–subunit interface some 12 Å from the allosteric site (residues 5–24 shown in orange with the Ser14-*P* displayed). The inhibitor site, which binds purine compounds such as caffeine (shown in green), is situated at the entrance to the catalytic site tunnel, formed by two hydrophobic residues of Phe285 and Tyr613 (the figure was produced using XOBJECTS, a molecular illustration programme; M.E.M. Noble, unpubl. results).

covery of over 80 Glc analogues inhibitors that have an increased affinity for GPb than Glc itself (K_i = 1.7 mM) (Tsitsanou et al., 1999, and references therein). The starting point for the rational design of these compounds was the X-ray crystal structure of T-state GPb-Glc complex. In recent work, W1807 (Scheme 1) was synthesized and found to be the most potent competitive inhibitor known of GPb with a K_i = 1.6 nM (with respect to AMP), a value which is 10^6-fold lower than the corresponding K_i for the physiological inhibitor Glc. A 2.3 Å resolution study of the cocrystallized GPb-W1807 complex revealed that W1807, which shows no chemical resemblance to any of the known regulators of GP, binds at the allosteric effector site of T-state GPb (Zographos et al., 1997) and induces conformational changes characteristic of the T′ state (Johnson et al., 1993). In more recent work, an inhibitor of human liver GPa, CP-91149 (Scheme 1), has been identified and characterized in vitro and in vivo (Martin et al., 1998). This compound was shown to be a potent inhibitor of human liver GPa with an IC_{50} of 1 μM and to be synergistic with both Glc and caffeine. CP-91149 was also shown to lower plasma Glc concentration in an animal model of Type 2 diabetes.

In this work, we present a detailed understanding of the regulation of GPa activity through kinetic and X-ray binding studies with the W1807 compound. To improve the precision of our understanding of the molecular basis of its potent inhibitory action on phosphorylase, the GPa-Glc, and GPa-Glc-W1807 cocrystallized complexes were analyzed at 2.0 and 2.1 Å resolution, respectively. The detailed interactions of W1807 with the protein provide a structural explanation for the kinetic properties and show that W1807 is an inhibitor that stabilizes a different conformation that of Glc. To address a possible explanation for the allosteric inhibition of GPa by W1807, structural comparisons were undertaken with various structures of GPb and GPa and examined.

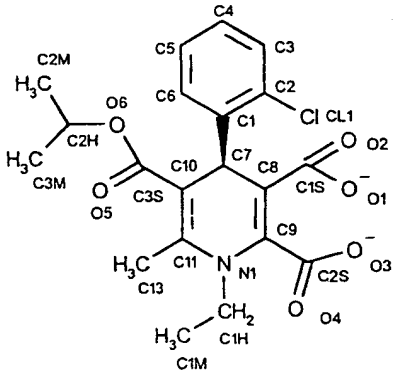

W1807

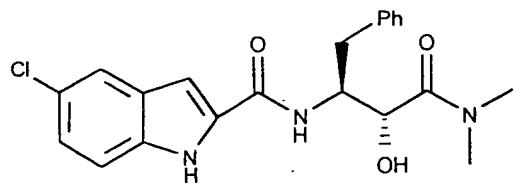

CP-91149

Scheme 1. W1807, showing the numbering system used, and CP-91149 (Martin et al., 1998).

Results

Kinetics

Kinetic experiments with GPa, in the absence of AMP, showed that W1807 is a potent inhibitor of the enzyme with a K_i = 10.8 nM competitive with Glc-1-*P* (Fig. 2). $K_{i,app}$ values for W1807 were 18.5, 24.0, 35.1, 58.2, and 130.5 nM, in the presence of 3, 4, 6, 10, and 20 mM Glc-1-*P*, respectively. Analysis of Lineweaver–Burk plots, obtained in the presence of constant concentration of AMP (1 mM) and glycogen (1%) and different concentrations of W1807 and Glc-1-P, showed that W1807 was also a competitive inhibitor of the enzyme with respect to Glc-1-*P* with an apparent K_i = 19.4 μM (Fig. 3). Both the Scatchard and the Lineweaver–Burk diagrams showed concave upward curvature, suggesting positive homotropic effects between substrate binding sites (in the terminology of Monod et al., 1965). To investigate the interaction if any between W1807 and Glc binding to GPa, initial velocity studies were carried out by varying W1807 and Glc concentrations at fixed concentrations of the substrate Glc-1-*P*. The kinetic data indicate that W1807 inhibition of GPa is synergistic with Glc, suggesting that both W1807 and Glc are able to bind to the enzyme at the same time (Segel, 1975). The effect of varying Glc concentration on the IC_{50} value for W1807 is shown in Figure 4. The IC_{50} value for W1807 inhibition is reduced from 88 to 22.7 nM in the pres-

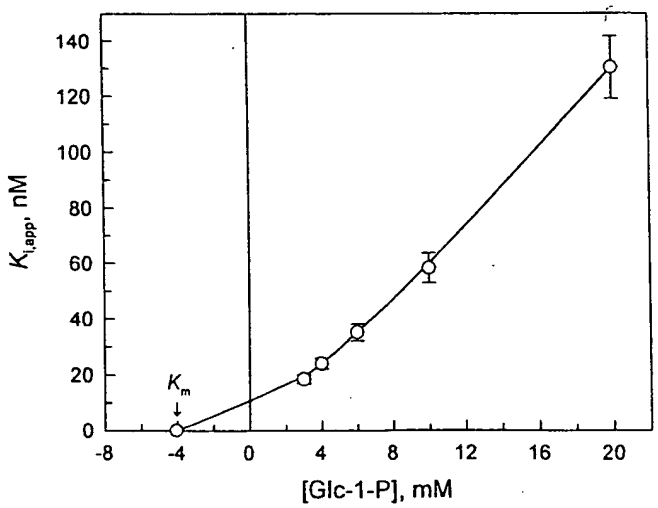

Fig. 2. The kinetics of GPa inhibition by W1807 with respect to Glc-1-*P* in the direction of glycogen synthesis. Effect of Glc-1-*P* concentration on the $K_{i,app}$ for W1807 inhibition of GPa. Kinetic data (in tetraplicate) obtained with 5 μg/mL GPa at a constant concentration of glycogen (1%) and various concentrations of the substrate Glc-1-*P* (3–20 mM) and inhibitor (60–140 nM) were analyzed using Scatchard plots. $[I]_{bound}$ for a given Glc-1-*P* concentration was calculated by the equation $[I]_{bound} = [E]_{total}(V_o - V_i)/V_o$, where $[E]_{total}$ is the total enzyme concentration, V_i is the initial velocity at a given Glc-1-*P* concentration in the presence of W1807, and V_o is the initial velocity in the absence of W1807. $K_{i,app}$ mean values (together with the standard deviations of the mean values, n = 4) plotted vs. Glc-1-*P* concentration yielded a curve from which an approximate K_i value of 10.8 nM can be calculated by extrapolation, assuming that W1807 is a competitive inhibitor with respect to Glc-1-*P* ($K_{i,app} = K_i(1 + [\text{Glc-1-}P]/K_m)$. The $K_{i,app}$ mean values were as follows: 18.5 ± 3.1 nM, 24.0 ± 3.9 nM, 35.1 ± 6.1 nM, 58.2 ± 10.8 nM and 130.5 ± 22.6 nM, in the presence of 3, 4, 6, 10, and 20 mM Glc-1-*P*, respectively. Enzyme exhibited a V_{max} value of 84.8 ± 2.7 μmol mg^{-1} min^{-1} (with respect to Glc-1-*P*) and a K_m value of 4.1 ± 0.3 mM for Glc-1-*P* at saturating glycogen (1%).

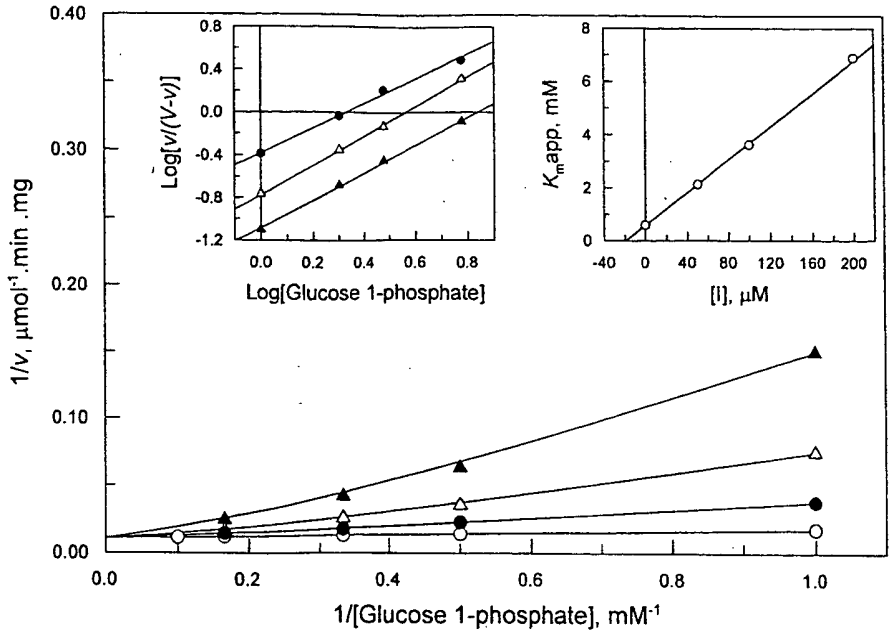

Fig. 3. Kinetics of W1807 inhibition of GPa with respect to Glc-1-*P* in the presence of AMP. Double reciprocal plots for GPa at constant concentrations of AMP (1 mM) and glycogen (1%) and various concentrations of inhibitor. Inhibitor concentrations were as follows: 0 (○), 50 (●), 100 (△), and 200 μM (▲). **Inset** (top left): Kinetic data were transformed into Hill plots for Glc-1-*P*, which yielded the apparent K_m and Hill coefficients n. The apparent K_m values and the Hill coefficients (given in parentheses) were 0.60 ± 0.02 mM (n = 1.0), 2.1 ± 0.3 mM (n = 1.0), 3.6 ± 0.1 mM (n = 1.4), and 6.9 ± 0.2 mM (n = 1.3) at 0, 50, 100, and 200 μM, respectively. **Inset** (top right): From the secondary plot of the apparent K_m values versus inhibitor concentration, a K_i value of 19.4 ± 0.5 μM was calculated. The enzyme exhibited a V_{max} value of 91.1 ± 0.5 μmol mg^{-1} min^{-1} (with respect to Glc-1-*P*) at saturating glycogen (1%) and AMP (1 mM).

ence of 10 mM Glc. Caffeine, a strong T-state inhibitor of the enzyme (with a K_i value of 0.1–0.2 mM), is also known to be a competitive inhibitor with respect to Glc-1-*P* for GPa and to function with Glc in a synergistic mode (Kasvinsky et al., 1978), with each compound promoting the binding of the other (with an interaction constant α of 0.2). The effect of Glc on the potency of W1807 could be an important physiological feature of a liver GPa inhibitor, as it has been suggested for the pair CP-91149/Glc (Martin et al., 1998), because the decrease in inhibitor potency as Glc concentrations decrease in vivo should diminish the risk of hypoglycemia.

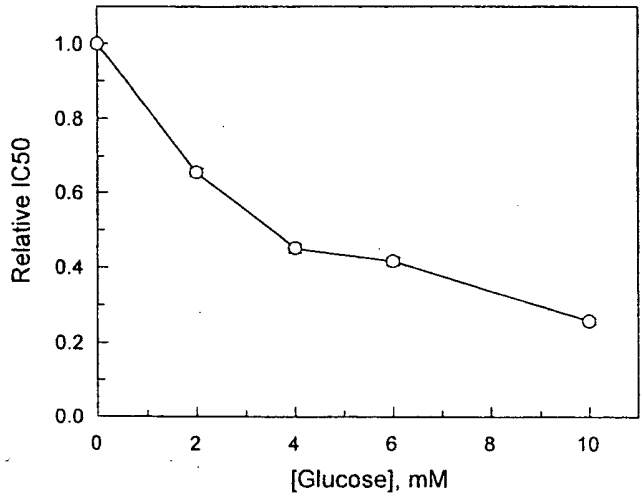

Fig. 4. The effect of Glc on the potency of W1807. IC_{50} values for GPa inhibition were determined in the direction of glycogen synthesis as described in Materials and methods with 5 μg/mL enzyme at constant concentrations of Glc-1-*P* (10 mM) and glycogen (1%), and varied W1807 concentrations (40–120 nM) in the absence or presence of various concentrations of Glc. The IC_{50} values were as follows: 88.3 ± 2.2, 58.0 ± 1.5, 39.8 ± 1.8, 36.8 ± 1.7, and 22.7 ± 1.3 nM in the presence of 0, 2, 4, 6, and 10 mM Glc, respectively. The normalized values (obtained by dividing these values by the IC_{50} value obtained in the absence of Glc) are plotted as a function of Glc concentration.

X-ray crystallography

Crystals of the T-state GPa can only be obtained in the presence of the allosteric inhibitor Glc (Fletterick et al., 1976). Similarly, crystals of the T-state GPa-Glc-W1807 complex were prepared in the presence of 50 mM Glc and 1 mM W1807. Crystallographic data collection at 100 K, processing and refinement statistics for the cocrystallized GPa-Glc and GPa-Glc-W1807 complexes, is shown in Table 1. For both complexes, the refined $2F_o - F_c$ electron density maps indicated that Glc bound at the catalytic site of GPa with the glucopyranose ring in chair geometry. Additional density at the allosteric site, in the GPa-Glc-W1807, indicated tight binding of W1807. There were also indications in both maps for binding of a glycerol molecule; glycerol was used as a cryoprotectant in both low temperature crystallographic experiments. The electron density for the Glc and the W1807 molecules as bound to the catalytic and allosteric sites, respectively, of T-state GPa are shown in Figures 5A and 5B.

Interactions between Glc and catalytic site residues

The mode of binding and the interactions that Glc makes with GPa in the absence or presence of W1807, at 100 K, are almost

Table 1. *Diffraction data and refinement statistics for T-state GPa-Glc and GPa-W1807-Glc complexes at 100 K*[a]

	GPa-Glc	GPa-Glc-W1807
Space group	$P4_32_12$	$P4_32_12$
No. of images (°)	60 (48°)	50 (50°)
Unit cell dimensions	$a = b = 127.2$ Å, $c = 116.2$ Å	$a = b = 127.2$ Å, $c = 115.8$ Å
Resolution	13.0–2.0 Å	13.0–2.1 Å
No. of observations	448,708	337,366
No. of unique reflections	57,879	51,612
$I/\sigma(I)$ (outermost shell)	14.62 (5.0)	11.35 (2.5)
Completeness (outermost shell)	90.1% (92.6%)	92.9% (87.3%)
R_m (outermost shell)	0.079 (0.410)	0.088 (0.242)
Outermost shell	2.03–2.00 Å	2.14–2.10 Å
Mosaicity	0.4	0.4
Refinement (resolution)	10.2–2.0 Å	13.0–2.1 Å
Residues included	5–250, 261–313, 325–838	5–250, 260–314, 325–835
No. of reflections used (free)	54,752 (2947 free)	48,964 (2648 free)
No. of protein atoms	6,617	6,603
No. of water molecules	807	753
No. of ligands atoms	15 (PLP)	15 (PLP)
	—	28 (W1807)
	12 (Glc)	12 (Glc)
	4 (Ser14-*P*)	4 (Ser14-*P*)
	6 (glycerol)	6 (glycerol)
Final R (%) (R_{free})	17.9% (23.0%)	18.9% (26.0%)
RMSD in bond lengths (Å)	0.008	0.008
RMSD in bond angles (°)	1.5	1.5
Average B (Å^2) for residues	5–250, 261–313, 325–838	5–250, 260–314,325– 835
Overall	23.5	28.9
CA,C,N,O	22.1	28.0
Side chain	24.8	29.7
Average B (Å^2) for ligands		
PLP	19.9	24.2
Water	—	—
W1807	—	26.5
Glc	22.7	25.9
Ser14-*P*	29.9	100.0
glycerol	32.9	33.3

[a]Merging R_m is defined as $R_m = \sum_i \sum_h |\langle I_h \rangle - I_{ih}| / \sum_i \sum_h I_{ih}$, where $\langle I_h \rangle$ and I_{ih} are the mean and ith measurement of intensity for reflection h, respectively. $\sigma(I)$ is the standard deviation of I. Crystallographic R-factor is defined as $R = \sum ||F_o| - |F_c|| / \sum |F_o|$, where $|F_o|$ and $|F_c|$ are the observed and calculated structure factor amplitudes, respectively. R_{free} is the corresponding R-value for a randomly chosen 5% of the reflections that were not included in the refinement.

identical with those previously reported for GPa (Sprang et al., 1982; Street et al., 1986) and those described for GPb (Martin et al., 1991) at room temperature. Glc on binding to GPa, in the absence of W1807, makes a total of 16 hydrogen bonds and 58 van der Waals interactions (3 nonpolar/nonpolar, 12 polar/polar, and 43 polar/nonpolar). In the GPa-Glc-W1807 complex, there are in total 17 hydrogen bonds, an additional rather long hydrogen bond (3.3 Å) is made between the α-1-OH and main-chain N of Leu136- and 65 van der Waals contacts (4 nonpolar/nonpolar, 14 polar/polar, and 47 polar/nonpolar). The structural results indicate that, in the presence of W1807, Glc can be accommodated at the catalytic site of GPa with essentially no disturbance of the structure (there are no significant differences in amino acid side chain positions) and the interactions it makes are similar to those observed in the GPa-Glc complex.

Interactions between W1807 and allosteric site residues

In the crystallization mixture, the W1807 concentration was 1.0 mM. The electron density suggests that the W1807 molecule is tightly bound at the allosteric site (Fig. 5B), consistent with the kinetic results. The position and conformation are similar with that observed for the refined structure of the T-state GPb-W1807 complex (Zographos et al., 1997). The allosteric site is situated where the C-termini of the helices α2 (residues 47–78) and α8 (residues 289–314) come together. It is lined by strands of the central core of β4 (residues 153–160) and β11 (residues 237–247), and surrounded on the third side by the sort β7 strand (residues 191–193) and the following loop to residue 197. The site is closed by the cap′ region (residues 36′ to 47′) from the symmetry-related subunit (superscript prime refers to residues from the symmetry-related subunit) and is some 35 Å from the catalytic site (Fig. 1).

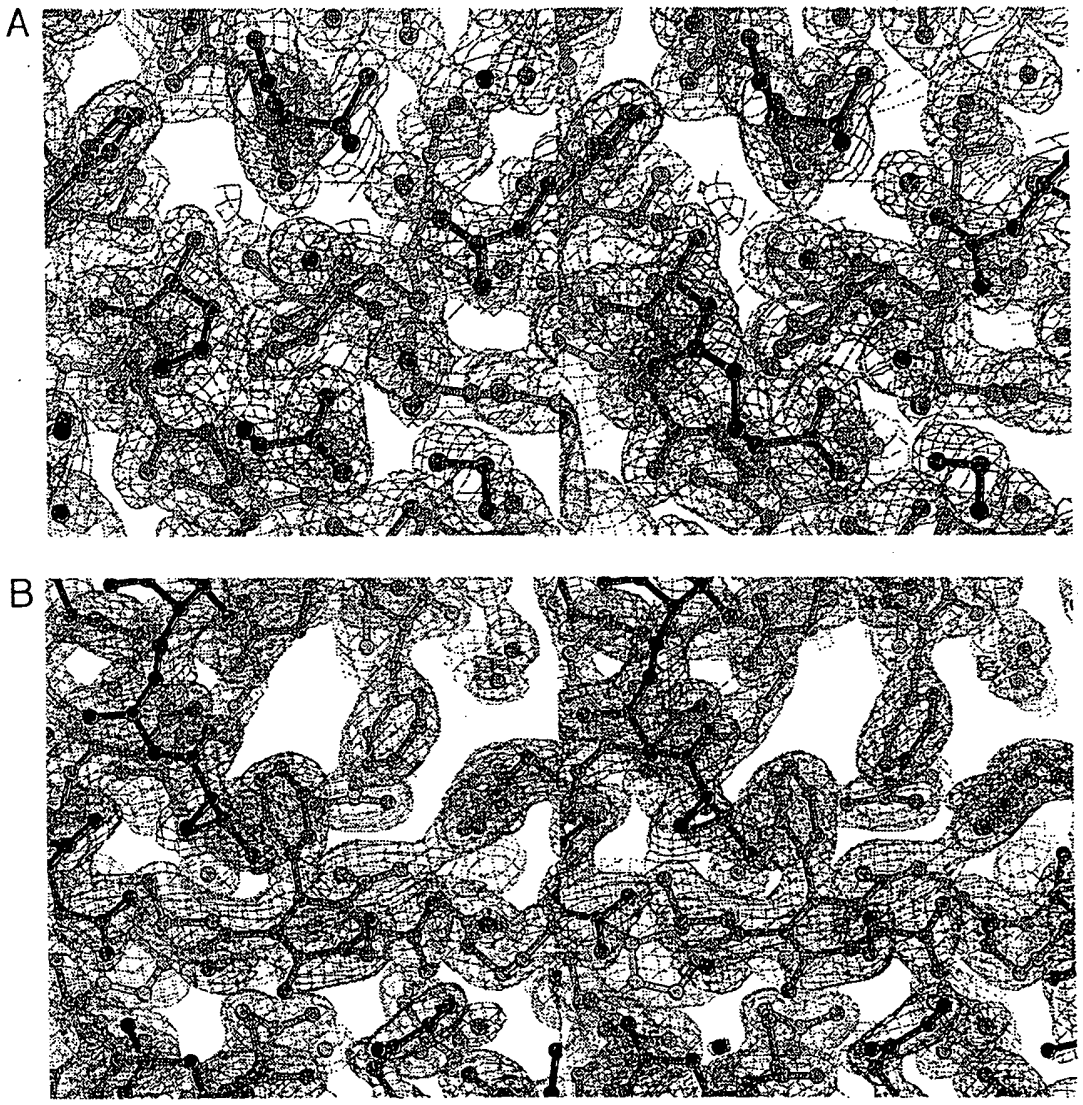

Fig. 5. Stereo diagrams of the catalytic and allosteric site of the refined GPa-Glc-W1807 complex, showing the bound (**A**) Glc and (**B**) W1807 and electron densities from the $2F_o - F_c$ maps. The contour levels correspond to ~1 RMSD of the maps (the figures were produced using XOBJECTS, a molecular illustration programme; M.E.M. Noble, unpubl. results).

The two subunits of the functional dimer associate at two positions located on opposite sides of the enzyme molecule. One contact, the cap′/α2 interface, is formed by the association of the cap′ with β7 strand and the α2 helix of the other subunit. An identical interface is produced by the molecular twofold symmetry operation. A second subunit–subunit contact involves the tower interface and consists of the antiparallel association of two symmetry-related helices, α7 (residues 262–276).

W1807 on binding at the allosteric site of GPa makes hydrogen bonds to suitable protein groups through each of the potential hydrogen bonding groups (except N1) of the molecule and numerous van der Waals contacts. In the GPa-Glc-W1807 complex structure, W1907 makes a total of 9 hydrogen bonds (Table 2; Fig. 6) and 67 van der Waals interactions of which 25 are interactions between nonpolar groups. The negative charge on the carboxylate groups is neutralized by ion pairing with three arginines, Arg242, Arg309, and Arg310, and hydrogen bonding with Gln71, Gln72, and Asp42′ through water molecules. Thus, carboxylate oxygen O1 makes a direct contact to Arg242 (NH2) and an indirect contact to Gln71 NE2 via a water molecule (Wat357). Carboxylate oxygen O2 makes two direct contacts with Arg309 (NH1) and Arg310 (NH2). Carboxylate oxygen O3 interacts directly with Arg309 (NH2) and Wat363, which in turn makes a direct contact to Ser313 O. Carboxylate O4 makes hydrogen bonds to the NE of Arg310 and Arg81 (via Wat564). Carbonyl oxygen O5 makes two indirect contacts with NE2 of Gln72 and OD2 of Asp42′ (from the symmetry-related subunit). The chlorine atom of the chlorophenyl group makes polar contacts to Arg193 and Asp227, and there is a short contact between CL1 and the guanidinium group NH2 group of Arg193 (2.8 Å) (but the corresponding distance in the GPb-W1807 complex is 3.6 Å). W1807 on binding at the allosteric site exploits numerous van der Waals contacts, which are dominated by the substantial nonpolar contacts to Val45′, Trp67, Ile68, Tyr75, and Phe196. These comprise mainly aromatic/aromatic interactions (chlorophenyl group/side-Phe196 side chain), CH/π electron interactions (methyl group/Tyr75 side chain, ethyl group/Tyr75 side chain, and Val45′ side chain/chlorophenyl group), and nonpolar/nonpolar interactions (isopropyl group/CD1 of Trp67,

Table 2. *Hydrogen bonds and van der Waals contacts between the W1807 and residues of the allosteric site of GPa*[a]

A. Hydrogen bonds

Inhibitor atom	Protein atom	Distance (Å)
O1	Wat357	2.5
	Arg242 NH2	3.3
O2	Arg309 NH1	2.5
	Arg310 NH2	2.7
O3	Arg309 NH2	3.0
	Wat363	2.7
O4	Arg310 NE	3.1
	Wat564	2.9
O5	Wat521	3.3

B. Van der Waals contacts

Inhibitor atom	Protein atom	No. of contacts
CL1	Arg193 CZ,NH2,CD; Asp227 OD2; Arg242 NH2; Wat409	6
O1	Arg242 CZ,NH1; Arg310 NH2	3
O2	Phe196 CE2; Arg242 NH1; Arg309 CZ,NH2; Arg310 NE,CZ	6
O3	Arg309 NH1,CZ; Arg310 CG,NE	4
O4	Ar81 NH2; Arg310 CG,CD; Wat363	4
O6	Gln71 CB,CG	2
C2	Phe196 CE2	1
C3	Glu195 OE1; Phe196 CE2; Lys41′ CE,NZ	4
C4	Glu195 OE1; Phe196 CE2,CZ; Lys41′ NZ	4
C5	Phe196 CE2,CZ; Val45′ CB,CG1	4
C10	Gln71 CB	1
C13	Gln71 C,O; Gln72 N,CA; Tyr75 CB; Wat521	6
C1S	Phe196 CE2; Arg309 NH1; Arg310 NH2; Wat357	4
C2S	Arg310 CG,NE; Wat363; Wat564	4
C3S	Gln71 CB	1
C1H	Tyr75 CB,CG,CD2	3
C2H	Ile68 CG1,CA	2
C1M	Tyr75 CD2; Wat351	2
C2M	Val40′ O; Lys41′ CA	2
C3M	Trp67 CD1,O; Gln71 CG; Wat409	4
Total		67

[a] Wat357 is in turn hydrogen bonded to Gln71 NE2 (bond distance = 3.0 Å); Wat363 is hydrogen bonded to Ser313 O (3.2 Å); Wat564 is hydrogen bonded to Arg81 NH1 (2.6 Å) and NH2 (3.2 Å); Wat521 is hydrogen bonded to Gln72 NE2 (3.3 Å) and Asp42′ OD2 (3.4 Å) (from the symmetry related subunit).

and CA and CG1 of Ile68, and aliphatic part of Gln71). In total, seven water molecules that are present in the native structure (GPa-Glc) are displaced on binding W1807 (Wat273, Wat517, Wat692, Wat695, Wat797, and waters Wat8 and Wat252 from the symmetry-related subunit), and one water, Wat14 (Wat409 in the GPa-Glc-W1807 structure), sifted to contact Asp227 OD2. The increase in entropy from the release of these waters, together with the van der Waals, halogen/polar, and the specific charge/charge interactions appear to be the major source of binding energy that results in an inhibitor with nM affinity for W1807 compared with mM affinity exhibited by Glc.

Comparison of 100 K and room temperature structures of T-state GPa in complex with Glc

The crystal structure of GPa in complex with the inhibitor Glc has been solved at 2.1 Å resolution at room temperature (Sprang et al., 1988). Although its quaternary structure is T-state, the conformation of residues at the Ser14-P site and the allosteric site (promoted by the Ser14-P and the N-terminal tail interactions) are almost identical to those observed in the R-state structure of GPa (Barford et al., 1991); both the N-terminal tail with Ser14-P is localized and the AMP site is in the high affinity state. However, the presence of Glc at the catalytic site of GPa prevents the prop-

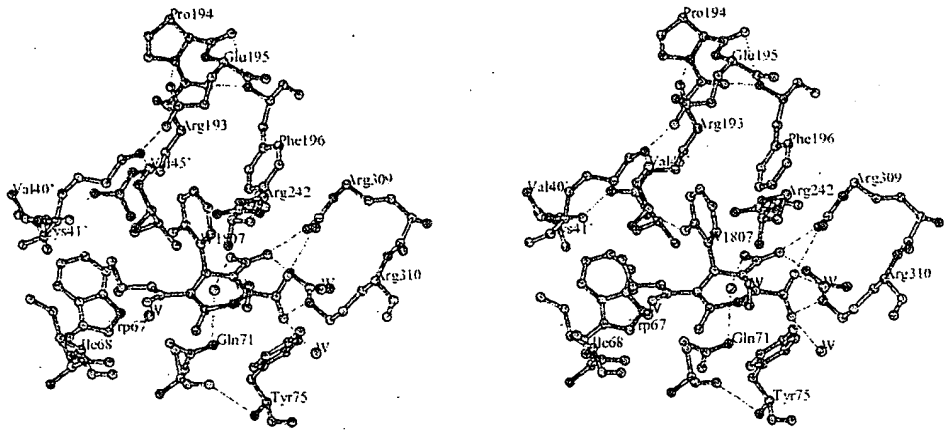

Fig. 6. The contacts between W1807 and GPa, viewed down the twofold axis. The view is similar to that shown in Figure 5B (the figure was produced using XOBJECTS, a molecular illustration programme; M.E.M. Noble, unpubl. results).

agation of conformational changes from the subunit interface to the catalytic site, and the GPa-Glc structure is considered to represent a conformation intermediate in the T → R transition in which the regulatory apparatus at the N-terminus has been decoupled from the catalytic site by Glc.

The 100 K GPa-Glc structure at 2.0 Å resolution is almost identical to the earlier room temperature GPa-Glc structure at 2.1 Å resolution (Sprang et al., 1988), except for the regions of high *B*-factors, and for certain side chains and flexible or surface loops that have slightly different conformations. Superposition of the 100 K and room temperature structures over well-defined regions (5–16, 22–249, 261–314, and 325–838) gave RMS deviations (RMSDs) of 0.314, 0.364, and 1.073 Å for Cα, main-chain, and side-chain atoms, respectively. Detailed examination showed that main-chain atoms of residues 16, 21–22, 127, 261, 325, 390, 434, 547, 552–557, 560, and 611–612 differed in position by more than 1.0 Å. These are mostly on the surface facing the solvent or have little associated electron density and high temperature factors.

Comparison between T-state GPa-Glc and T-state GPa-Glc-W1807 complexes

Superposition of the 100 K structures over well-ordered parts of the GPa-Glc structure (residues 5–250, 261–313, and 325–835) gave RMSDs of 0.348, 0.356, and 0.724 Å for Cα, main-chain, and side-chain atoms, respectively. The binding of W1807 to the allosteric site of the T-state GPa (in the presence of Glc) promotes extensive conformational changes. The major shifts for main-chain atoms are for residues 5 to 33 (between 0.5 to 2.2 Å), residues 36 to 43 (between 0.4 to 0.6 Å), residues 45 to 52 (between 0.6 and 1.2 Å), residues 63 to 77 (between 0.4 to 1.4 Å), residues 104 to 129 (between 0.4 to 1.5 Å), residues 183 to 186 (between 0.4 to 0.6 Å), and residues 192 to 196 (between 0.6 to 1.4 Å) that affect the subunit–subunit interface in the region between the cap′ (residues 36′ to 47′) and the loop between β7 (residues 191 to 193) and β8 (residues 198 to 209) strands. The binding of W1807 to GPa is accompanied by certain local conformational changes in the vicinity of the allosteric site. The greatest changes include shifts of the main-chain atoms of residues 193 to 196 by about 0.8 to 1.4 Å with the phenyl ring of Phe196 moving toward the chlorophenyl group by 3 Å, main-chain atoms of residues 71 to 77 by about 0.5 to 1.0 Å with the side chain of Tyr75 moving toward the ethyl group by 1 Å, and also shifts of the main-chain atoms of residues 45′ to 49′ of about 0.7 to 1.2 Å. There are no changes at the catalytic site or at the tower/tower′ helix subunit interface.

In the GPa-Glc structure, the N-terminal segment (residues 5–22), which contains the phosphorylation site, folds into a distorted 3_{10} helix and make intersubunits contacts. The Ser14-*P* makes ionic contacts with two arginine residues, Arg69 from its own subunit and Arg43′ from the other (symmetry-related) subunit. There are intersubunit hydrogen bonds between Arg10 and the carbonyl oxygen atom of residue Gly116′, between NE2 of Gln12 and NZ of Lys28′ and main chain O of Gln114′, between main chain O of Ile13 and NH1 of Arg43′, between main chain O of Ser14 and ND2 and OD1 of Asn3′ and NE2 of His36′. The nonpolar residues that flank the Ser14, Ile13, and Val15 dock into hydrophobic pockets formed from the side chains of Leu35′ and Arg43′, and Tyr51′ and from the side chains of Ile68, Arg69, and His36′, respectively. In the GPa-Glc-W1807 complex structure, the N-terminal tail, residues 5–22, is difficult to locate. Examination of the electron density in this region indicates that there is poor density for Ser5, Gln7, Glu8, Lys9, Arg10, Gln12, Ile13, the Ser14-P group, Val15, Leu18, and Glu22, but no electron density is observed for residues Asp6, Lys11, Ser14, the Ser14-P group oxygens, Arg16, Gly17, and Ala19, Gly20, and Val21. Indeed, residues 5–22 are the most disordered residues of the GPa-Glc-W1807 complex structure. When modeled and included in the refinement, residues 5–26 showed overall ⟨*B*⟩-factor values of 94.4 Å^2 (with a value of 100.0 Å^2 for Ser14-*P*).

In the GPa-Glc complex structure, there are hydrogen bonds across the subunit interface in the vicinity of the allosteric site that are important in maintaining the dimer structure. Arg193 hydrogen bonds to the main-chain oxygens of residues Leu39′ (2.9 Å), and Val40′ (2.8 Å), and Glu195 hydrogen bonds to Ly41′ (2.5 Å). These contacts are present in both T- and R-state enzymes. On forming the complex with W1807, the major shift in residues 193 to 196 affects the positions of key subunit interface residues. However, the intersubunit hydrogen bonding pattern is not changed. Arg193 hydrogen bonds to the main chain O of Leu39′ (3.1 Å), and Val40′ (2.7 Å), and Glu195 is still able to hydrogen bond to Lys41′ (2.8 Å) because of compensatory shifts. The Tyr185′/Pro194 contact, which is an important subunit/subunit contact and a major link between the cap′/α2 and the tower/tower′ contacts, is also retained in the W1807 complex.

Comparison of the GPa-Glc-W1807 complex with the GPa-Glc complex structure indicated that the two structures could be superimposed after a transformation that corresponded to a rotation of 1.2° and a translation of 0.57 Å of the GPa-Glc-W1807 complex relative to the GPa-Glc complex structure such that one subunit was brought closer to the other across the twofold axis (which in the T-state crystal is also a crystallographic twofold axis of symmetry) (Table 3).

Comparison between T-state GPb-W1807 and T-state GPa-Glc-W1807 complexes

The electron density map of the GPa-Glc-W1807 complex structure indicated that W1807 binds in the same orientation and conformation with that of W1807 in the GPb-W1807 complex structure (Zographos et al., 1997) and the interactions formed by the functional groups of the W1807 at the allosteric site are essentially identical. Having superimposed the structures of the two complexes, it became apparent that they closely resemble. The binding of W1807 in the T-state GPb crystals is accompanied by substantial conformational changes. The shifts in the region of 43′ to 49′ and 192 to 196 affect residues remote from the allosteric site (such as Pro194), which in turn affect the subunit/subunit interface packing (Zographos et al., 1997). The enzyme shows a small rotation (1.6°) (Table 3), this rotation bringing the two subunits of the dimer closer together. In the GPb-W1807 complex, residues 43′ to 49′ move closer to the other subunit and tighten the W1807 site, while residues 192 to 196 shift to contribute (through Phe196) van der Waals′ interactions. These shifts appear important in stabilizing a modified T-state, denoted T′, that is "more T-state than the T-state." It is remarkable that exactly the same shift is observed on binding W1807 to the allosteric site of GPa, and this indicates that binding of W1807 to the allosteric site of GPa promotes a similar conformational state. The binding of W1807 to both forms of the enzyme appears to stabilize similar conformations. The LSQKAB comparison of the structure of the GPb-W1807 complex with the structure of the GPa-Glc-W1807 complex showed that the positions of the Cα and main-chain atoms for residues 13–250, 260–314, and 325–835 deviate from their mean positions by 0.262 and 0.289 Å, respectively, indicating that the complexes are similar in their overall conformation to within the limits of the 2.3 Å resolution data.

Comparison between T-state GPa-Glc-AMP and T-state GPa-Glc-W1807 complexes

The structure of the Glc-inhibited GPa bound to AMP with data extending to 2.5 Å resolution has been described (Sprang et al., 1987). The binding of AMP to the GPa-Glc tetragonal crystals has been shown to be more characteristic of the activated (R) state of the enzyme. The superposition of the structure of the T-state GPa-Glc-AMP complex with the structure of the T-state GPa-Glc-W1807 complex over residues 5–15, 24–249, 261–314, 325–835 gave RMSDs of 0.532, 0.559, and 1.236 Å for Cα, main-chain, and side-chain atoms, respectively. Comparison of the GPa-Glc-AMP complex with the GPa-Glc-W1807 complex structure by superimposition of the activation loci of both subunits of the dimers followed by determination of the transformation needed to best superimpose the subunits, indicated that each subunit rotates by 1.0° (relative to GPa-Glc-W1807 subunits) about an axis that is nearly perpendicular to the molecular dyad (Table 3). Modeling studies suggest that the allosteric site of the T-state GPa-Glc-AMP complex cannot allow W1807 to bind unless residues Tyr75, Gln71, and Val45′, which otherwise would make unfavorable contacts to the inhibitor, change the (χ1,χ2) angles as follows: Tyr75 (χ1 from −88 to 179°; χ2 from −67 to −108°), Gln71 (χ2 from 159 to −50°), and Val45′ (χ1 from 65 to −67°).

Comparison with R-state GPa

Superposition of the structure of the R-state GPa (subunit A) with the structure of the GPa-Glc-W1807 complex gave RMSDs of 1.251, 1.261, and 2.119 Å for C_α, main-chain and side-chain atoms, respectively, for residues 10 to 250, 260 to 314, and 325 to 835.

Table 3. *Comparison between various phosphorylase structures with respect to the relative orientation of subunits*[a]

Structures	Displacement, RMS (Å)	Rotation, χ (Å)
T-state GPa-Glc-W1807 vs. T-state GPa-Glc	0.348	1.2
R-state GPa vs. T-state GPa-Glc-W1807	1.251	4.8
T-state GPb-W1807 vs. T-state GPa-Glc-W1807	0.262	0.0
T-state GPa-Glc-AMP vs. T-state GPa-Glc-W1807	0.532	1.0
R-state PLPP-GPb-AMP vs. T-state GPa-Glc-W1807	1.217	4.5
T-state GPb vs. T-state GPb-W1807	0.440	1.6
R-state GPb-AMP vs. T-state GPa-Glc-W1807	1.076	4.9

[a]RMSDs in Cα positions and subunit rotations were determined following the method of Sprang et al. (1991) using the program LSQKAB (CCP4, 1994). Structural units (N-domain core, C-domain core, and activation locus) were those defined previously (Sprang et al., 1991). Subunit rotation (χ) describes the rotation about an axis positioned near the central interface (residues 185 to 194) that is nearly perpendicular to the twofold axis of the dimer. Structures T-state GPa-Glc, T-state GPa-Glc-W1807, T-state GPb-W1807, T-state GPa-Glc-AMP, T-state GPb, R-state PLPP-GPb-AMP, R-state GPa, and R-state GPb-AMP correspond to the T-state GPa-Glc complex (this work), the GPa-Glc-W1807 complex (this work), the T-state GPb-W1807 complex (Zographos et al., 1997), the T-state GPa-Glc-AMP complex (Sprang et al., 1987), the T-state GPb (Gregoriou et al., 1998), the PLPP-GPb-AMP complex (Sprang et al., 1991), the R-state GPa (Barford et al., 1991), and the R-state GPb-AMP complex (Barford et al., 1991), respectively.

The transformation (obtained with LSQKAB) that allows superposition of the structures R-state GPa to T-state GPa-Glc-W1807 is similar to the transformations that allow superposition of R-state GPa to T-state GPa-Glc and R-state GPa to T-state GPb. These involve a rotation of one subunit by about 5° so as to bring the two subunits closer together at the twofold axis of the dimer. Modeling studies suggest that if W1807 were to be incorporated into the allosteric site of the R-state GPa structure, the site could accommodate W1807 but that it would bind with fewer contacts. Obviously, some alteration in the region of the allosteric site is necessary to allow W1807 to bind tightly. In particular, residues 192–196 would be required to shift toward the inhibitor to provide the contacts to the chlorophenyl ring but such a shift would be resisted by the subunit–subunit contacts that promote the R-state.

Comparison with R-state PLPP-GPb-AMP

Superposition of the R-state PLPP-GPb-AMP complex structure (subunit A) with T-state GPa-Glc-W1807 structure over regions 24–249, 264–276, 289–313, and 325–835 gave RMSDs of 1.217, 1.218, 1.897 Å for Cα, main-chain, and side-chain atoms, respectively. Unlike the allosteric site of R-state GPa complex that would be able to accommodate W1807 without any significant change in structure, the binding of W1807 at the allosteric site of PLPP-GPb-AMP complex would require a change in the $\chi 1$ angle of Tyr75 and $\chi 2$ angle of Trp67 from −78° and 86° to 179° and 1°, respectively.

Figures 7 and 8 show details of the contacts made at the allosteric site and the subunit/subunit interface (residues at the cap′ and the start of the $\alpha 2'$ helix and the $\beta 7$–$\beta 8$ loop) for T-state GPb-W1807 complex, T-state GPa-Glc complex, R-state GPa, T-state GPa-Glc-AMP complex, R-state GPb-AMP complex, and PLPP-GPb-AMP complex. With the exception of the T-state GPb-W1807 complex, the shifts for the residues 39′–52′, 67–68, 71, 75, 181′–185′, and 193–196 in all complexes compared with the GPa-Glc-W1807 complex are apparent, but the magnitude of both the tertiary and quaternary conformational changes differ in the various structures.

Discussion

It is generally considered that GPa has escaped some of the allosteric properties of GPb. The allosteric constant L (the equilibrium constant for the transition between the R- and T-states, $L = [T_0]/[R_0]$) for GPb is at least 3,300 and for GPa is between 3–13 (evidence in Madsen, 1986). Thus, the AMP/ATP effects on GPa activity are far less pronounced than for GPb where ATP directly competes for AMP, an obligate allosteric activator. The activity of GPb can be enhanced from 0–1% to about 80% of that of GPa by AMP, whereas there is only a 10–20% increase in GPa activity by AMP. In addition, it has been suggested that it is only this "added" activity that ATP inhibits (Fletterick & Madsen, 1980). The most naturally occurring inhibitor of GPb is Glc-6-P, which in the muscle cell serves to maintain the enzyme in the T-state unless activated by AMP or by phosphorylation to give GPa. Glc-6-P exhibits a K_i of 0.25 mM when competing with AMP (Oikonomakos et al., 1995b). GPa is not appreciably inhibited by Glc-6-P, but it is inhibited at nonphysiological concentrations (Melpidou & Oikonomakos, 1983). Fletterick and Madsen (1980) have assumed that GPa inhibition by Glc-6-P is analogous to the ATP inhibition with both acting at the AMP site. Whether or not GPa can be inhibited by an inhibitor binding at the AMP site has remained an unanswered question.

On the basis of our observations, we show that the binding of W1807 at the activator AMP site of GPa inhibits the binding of the substrate Glc-1-*P* allosterically. This is, to our knowledge, the first direct evidence of GPa allosteric inhibition through ligand binding at the allosteric site. W1807, on binding to GPa, occupies a similar position to that observed for the AMP (Sprang et al., 1987) except that the position of the chlorophenyl ring component is quite different from the adenine of AMP (Figs. 7C, 8C). It therefore seems probable that the lower affinity of W1807 for GPa in the presence of AMP obtained in the kinetic experiments (Fig. 3) can be explained because AMP ribose and phosphate group and the W1807 isopropyl and carboxylate groups use distinct but mutually exclusive binding sites. Since both ligands must use these components to bind, any ternary complex of the type GPa-AMP-W1807 is unlikely to exist.

A comparison of T-state GPa-Glc-W1807 and R-state GPb and GPa structures can reveal the predominant key interactions and conformational changes associated with W1807 binding to the allosteric site of GPa. The chlorophenyl, isopropyl, and ethyl groups of W1807 make extensive nonpolar interactions with the enzyme that involve the aromatic groups of Phe196, Try67, and Tyr75, respectively, in addition to other side chains. The pyridine-5,6-dicarboxylate groups contact three arginine residues at the phosphate recognition site of the allosteric site. Modeling studies suggest that the binding of W1807 to the R-state GPa would not result in any unfavorable contacts at the allosteric site. Although such a hypothesis would need to be confirmed by experimental measurement, the results suggest that W1807 on binding stabilizes the T′-state by formation of van der Waals contacts, hydrogen bonds, and ion pairs. The mechanism of binding of W1807 to GPa is a clear example of induced fit. Enzyme overall structure is altered by the binding of a small ligand. It seems likely that the formation of a stable ligand-protein complex requires conformational changes in the vicinity of the allosteric site, particularly in the backbone and side chain of residues 192 to 196 and in the cap′ region of the other subunit (residues 43′ to 49′) and some small quaternary structural changes. The key interaction is probably the backbone displacement of the loop 192–196 to make van der Waals interactions with seven atoms of the ligand. W1807, therefore, upon binding to GPa results in additional favorable contacts with the enzyme. This may account for the observed specificity of GP for W1807. One of the most significant differences between T-state GPa-Glc and T-state GPa-Glc-W1807 complexes lies in that the N-terminal tail that carries the Ser14-*P* cannot be located in the electron density map of the W1807 complex structure and is assumed to undergo a conformational shift. The structural results show that there are changes that affect the subunit–subunit contacts that are important in allosteric effects (Fig. 8). Unlike activation by phosphorylation, where the N-terminal residues shift with a change in conformation from mobile to ordered, which is accompanied by changes in the tertiary and quaternary structure that lead to activation at the catalytic site, 45 Å away from the Ser14-*P* site, once W1807 is bound at the allosteric site it triggers transmission of effects that lead to inhibition in the muscle enzyme by favoring the R- to T-state transition of the enzyme.

The crystallographic analysis of the W1807 complex has shown that diversity in ligand binding can be achieved with small conformational shifts. The ability of GP to distinguish between AMP

(or ATP) (Sprang et al., 1987), Glc-6-*P* (or 2-deoxy-Glc-6-*P*)(Johnson et al., 1993; Oikonomakos et al., 1995b), and W1807 (Zographos et al., 1997; this work) appears to originate in protein flexibility in the region of the allosteric site, which result in additional protein:ligand interactions. The different binding modes of the AMP (or ATP) and Glc-6-*P* (or 2-deoxy-Glc-6-*P*) and the different contacts made to the enzyme compared to W1807 show a remarkable degree of plasticity for the allosteric site. This is a remarkable degree of versatility for a binding site, which is able to recognize specifically dissimilar compounds by employing the same

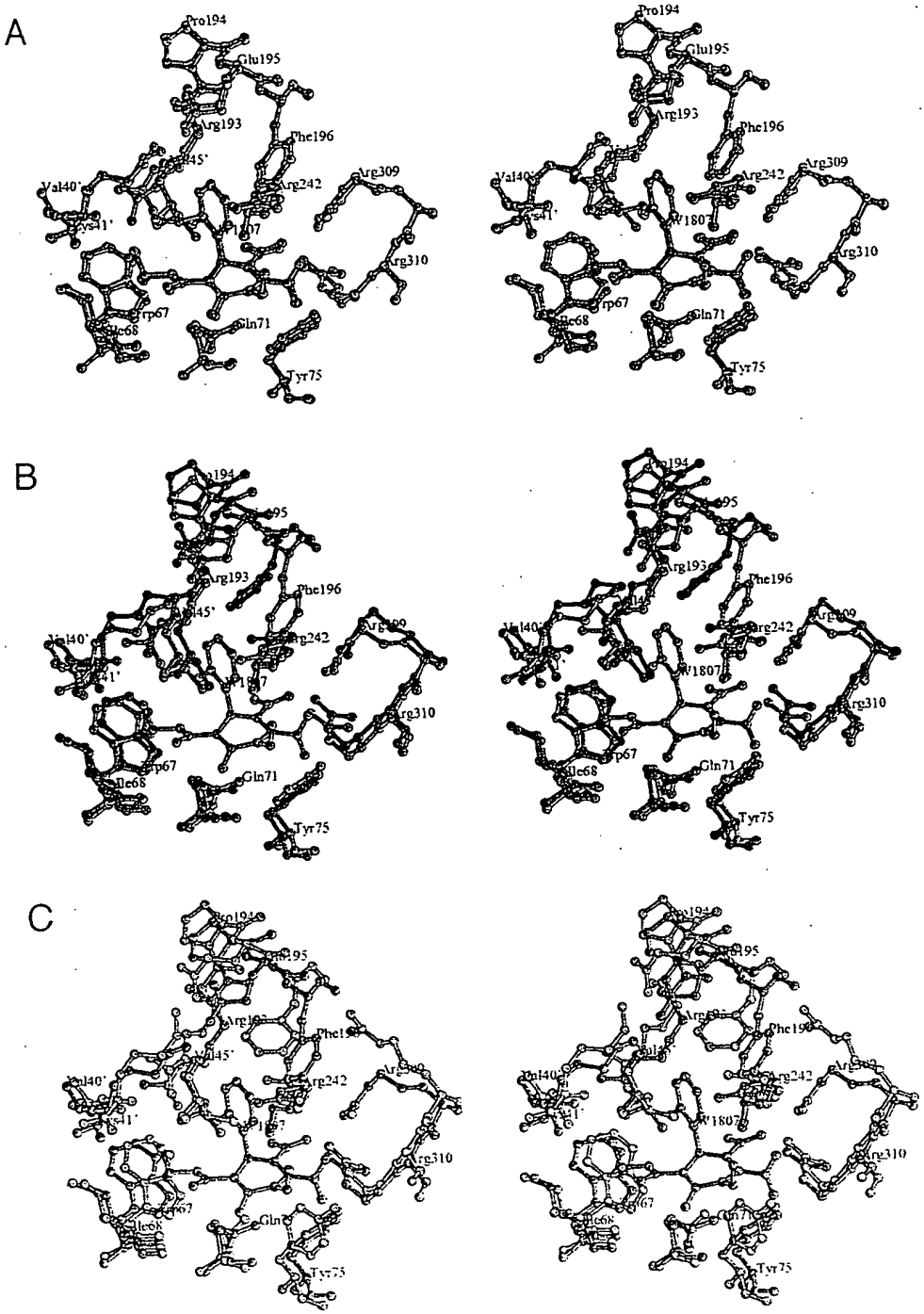

Fig. 7. The W1807 binding site in GPa. The view is similar to that of Figure 6. The W1807 binding site (in T-state GPa-Glc-W1807 complex) with that of (**A**) W1807 in the T-state GPb-W1807 complex, (**B**) the W1807 binding site with the allosteric site of T-state GPa-Glc complex, (**C**) the W1807 binding site with the allosteric site of R-state GPa, (**D**) the W1807 binding site with that of AMP in T-state GPa-Glc-AMP complex, (**E**) the W1807 binding site with that of AMP in the R-state GPb-AMP complex, and (**F**) the W1807 binding site with that of AMP in the PLPP-GPb-AMP complex superimposed are shown in stereo. Green, T-state GPa-Glc-W1807 complex; red, T-state GPb-W1807 complex; blue, GPa-Glc complex; magenta, R-state GPa; orange, T-state GPa-Glc-AMP complex; cyan, R-state GPb-AMP complex; red-brown, PLPP-GPb-AMP complex (the figures were produced using XOBJECTS, a molecular illustration programme; M.E.M. Noble, unpubl. results). (*Figure continues on facing page.*)

residues. Understanding such protein conformational flexibility will be important in the design and optimization of inhibitors.

In conclusion, the X-ray crystallographic study of the GPa-Glc-W1807 complex showed that W1807 binds at the allosteric site, the site that binds AMP, at the subunit–subunit interface of the dimer, and induces conformational changes characteristic of a T′-state conformation. The detailed interactions of W1807 with the protein provide a structural explanation for the potency of W1807 as an allosteric inhibitor of GPa and show that W1807 can stabilize a different conformation that of Glc. On binding to the allosteric site, W1807 is able to inhibit AMP binding directly and substrate Glc-1-*P* binding indirectly by stabilizing the T′ state. The results with W1807 (this work) and with CP-91149 (Martin et al., 1998) show how nonphysiological compounds can be potent inhibitors of glycogen degradation. Furthermore, structural analyses can be further exploited (by means of new chemical modifications) to produce other potential compounds that could be developed as antidiabetic agents.

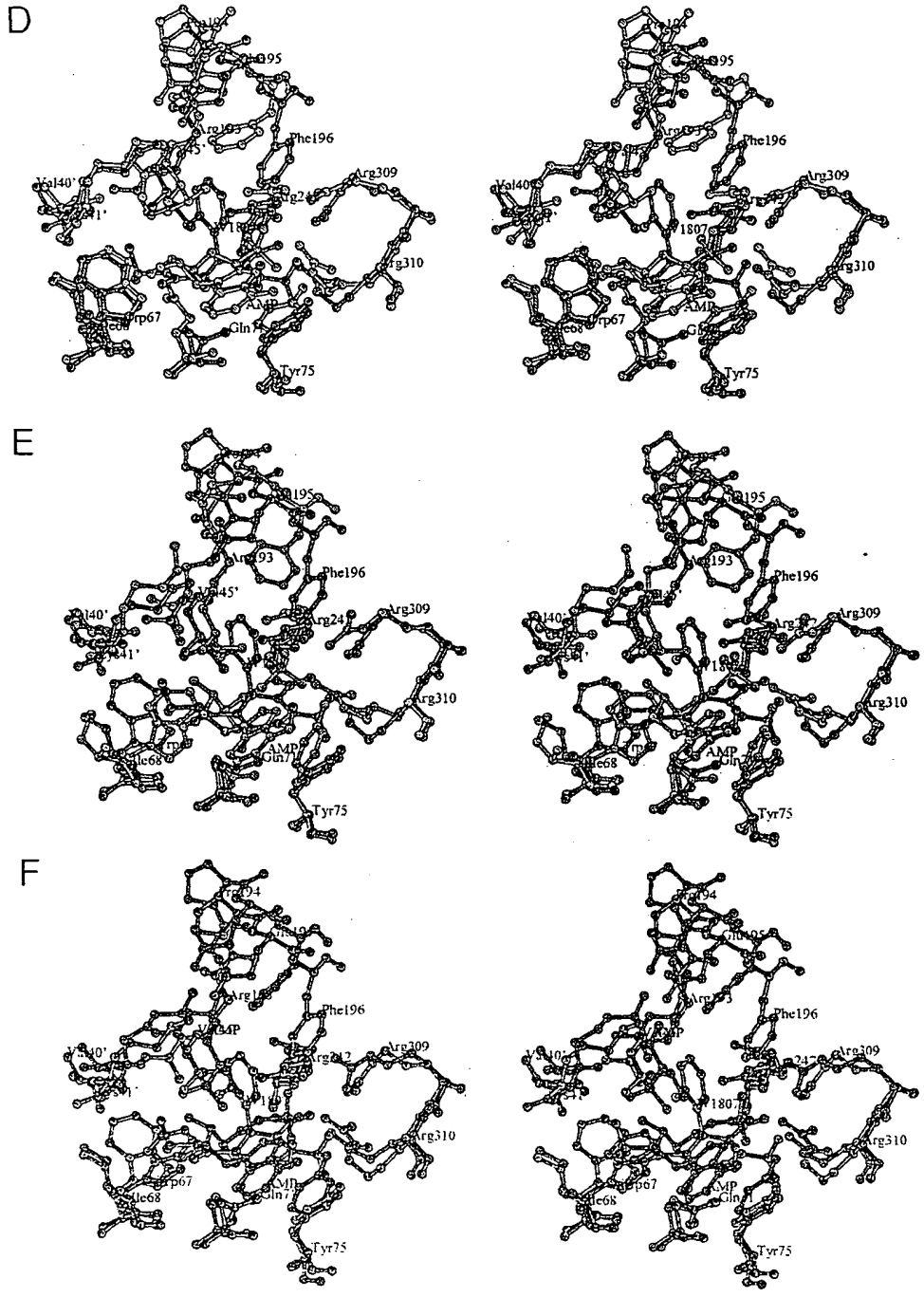

Fig. 7. *Continued.*

Materials and methods

Kinetic studies

GPb was isolated from rabbit skeletal muscle according to Fischer and Krebs (1962) using 2-mercaptoethanol instead of L-cysteine and recrystallized at least four times. GPa was prepared from GPb by phosphorylation according to the method of Cohen (1973) using an active phosphorylase kinase γ subunit truncated form (comprising residues 1–298), prepared as described (Owen et al., 1995), instead of phosphorylase kinase holoenzyme. GPa was recrystallized two times and bound nucleotides were removed from the enzyme as previously described (Melpidou & Oikonomakos, 1983). Protein concentration was determined from absorbance measurements at 280 nm using an absorbance index $A^{1\%}_{1cm}$ = 13.2 (Kastenschmidt et al., 1968). Calculations of GPa molarity were based on a MW of 97,434 (Johnson et al., 1989). Glc-1-*P* (dipotassium salt), AMP, (oyster) glycogen, and other chemicals were obtained from Sigma Chemical Company (St. Louis, Missouri). Glycogen was freed of AMP by the method of Helmreich and Cori (1964). Initial reaction rates were measured at pH 6.8 and 30 °C in the direction of glycogen synthesis as previously (Oikonomakos et al., 1995a).

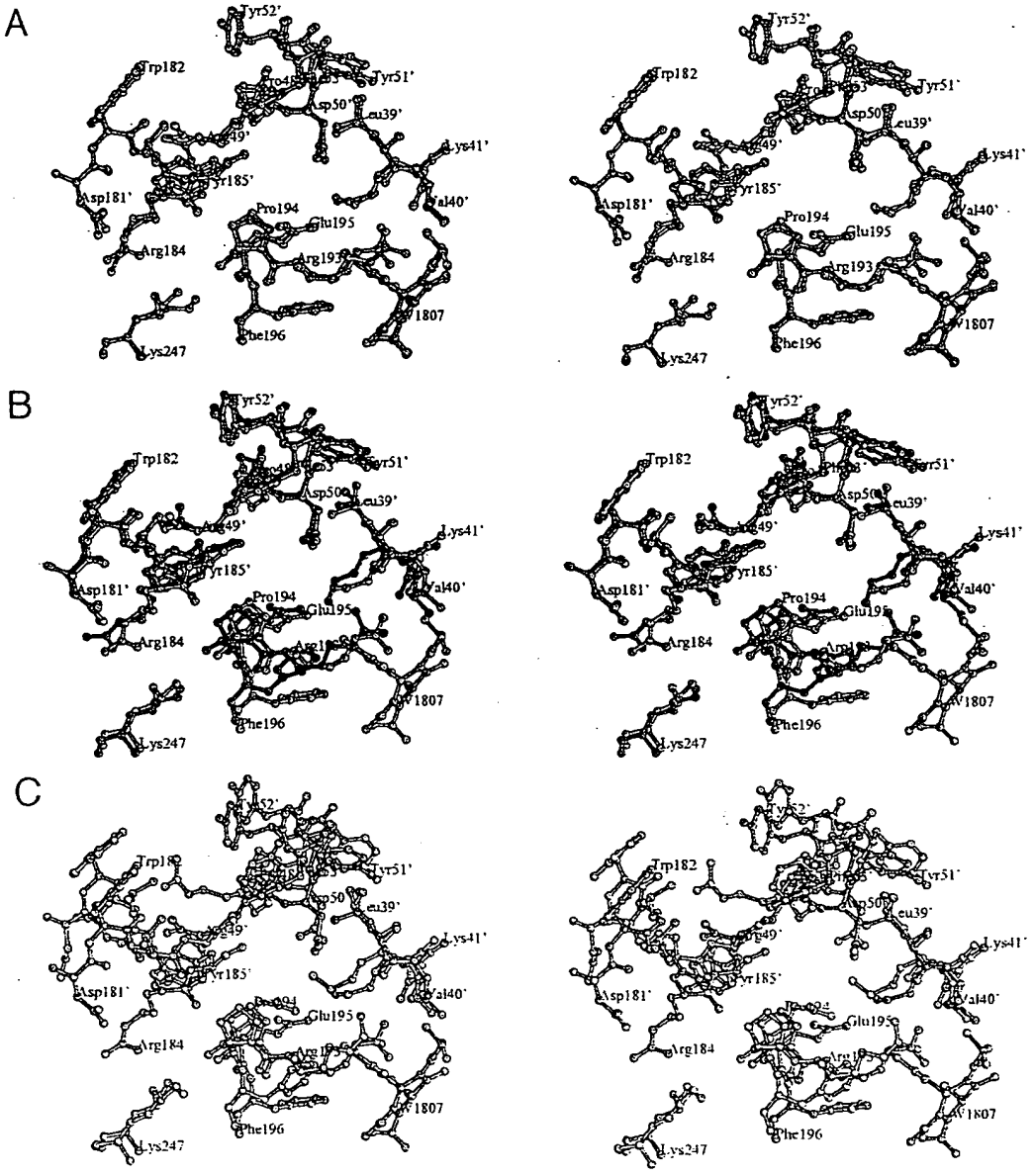

Fig. 8. Superposition of residues from the subunit–subunit interface in the GPa dimer. T-state GPb-W1807 complex superimposed onto the (A) T-state GPa-Glc-W1807 complex, (B) T-state GPa-Glc complex superimposed onto the T-state GPa-Glc-W1807 complex, (C) R-state GPa superimposed onto the T-state GPa-Glc-W1807 complex, (D) GPa-Glc-AMP complex superimposed onto the T-state GPa-Glc-W1807 complex, (E) R-state GPb-AMP complex superimposed onto the T-state GPa-Glc-W1807 complex, and (F) PLPP-GPb-AMP complex superimposed onto the T-state GPa-Glc-W1807 complex are shown in stereo. Green, T-state GPa-Glc-W1807 complex; red, T-state GPb-W1807 complex; blue, GPa-Glc complex; magenta, R-state GPa; orange, T-state GPa-Glc-AMP complex; cyan, R-state GPb-AMP complex; red-brown, PLPP-GPb-AMP complex (the figures were produced using XOBJECTS, a molecular illustration programme; M.E.M. Noble, unpubl. results). (*Figure continues on facing page.*)

Crystallographic studies

Crystallization and data collection

T-state GPa crystals were prepared essentially as described previously (Fletterick et al., 1976) and crystals of GPa-Glc-W1807 complex were grown, similarly, with 1 mM Bayer W1807. Just before data collection, the crystals were transferred to a fresh buffer solution (50 mM Glc, 10 mM magnesium acetate, 3 mM DTT, 10 mM Bes, 0.1 mM EDTA, 0.02 % sodium azide, pH 6.7, with or without 1 mM W1807) containing 30% v/v glycerol for 30–60 s prior to mounting in a loop, and flash frozen (100 K). Data were collected from single crystals using a 18 cm diameter MAR Research (Hamburg, Germany) image plate system, which was mounted on the beamline X-ray diffraction (λ = 1.0 Å) at ELETTRA (Trieste, Italy). Data frames of 0.8–1.0° oscillation angle were collected over total angular ranges of 48–50°. Crystal orientation, integration, and data reduction were performed using DENZO and SCALEPACK (Otwinowski, 1993).

Refinement

Crystallographic refinement of the 100 K native GPa-Glc complex soaked with 30% glycerol was performed with X-PLOR version 3.8 (Brünger, 1996) using bulk solvent corrections. The starting protein structure was the 2.1 Å refined model of the room temperature native GPa-Glc (with water molecules removed) (Sprang et al., 1988) kindly provided by Prof. R.J. Fletterick. Map interpretation using the program O (Jones et al., 1991) into difference density maps ($F_o - F_c$ and $2F_o - F_c$) showed strong density for Glc bound at the catalytic site. Several side chains of the enzyme model were adjusted, a model of Glc was fitted to the density at the catalytic site, and water molecules were built and retained only if they met stereochemical requirements. The final model was then

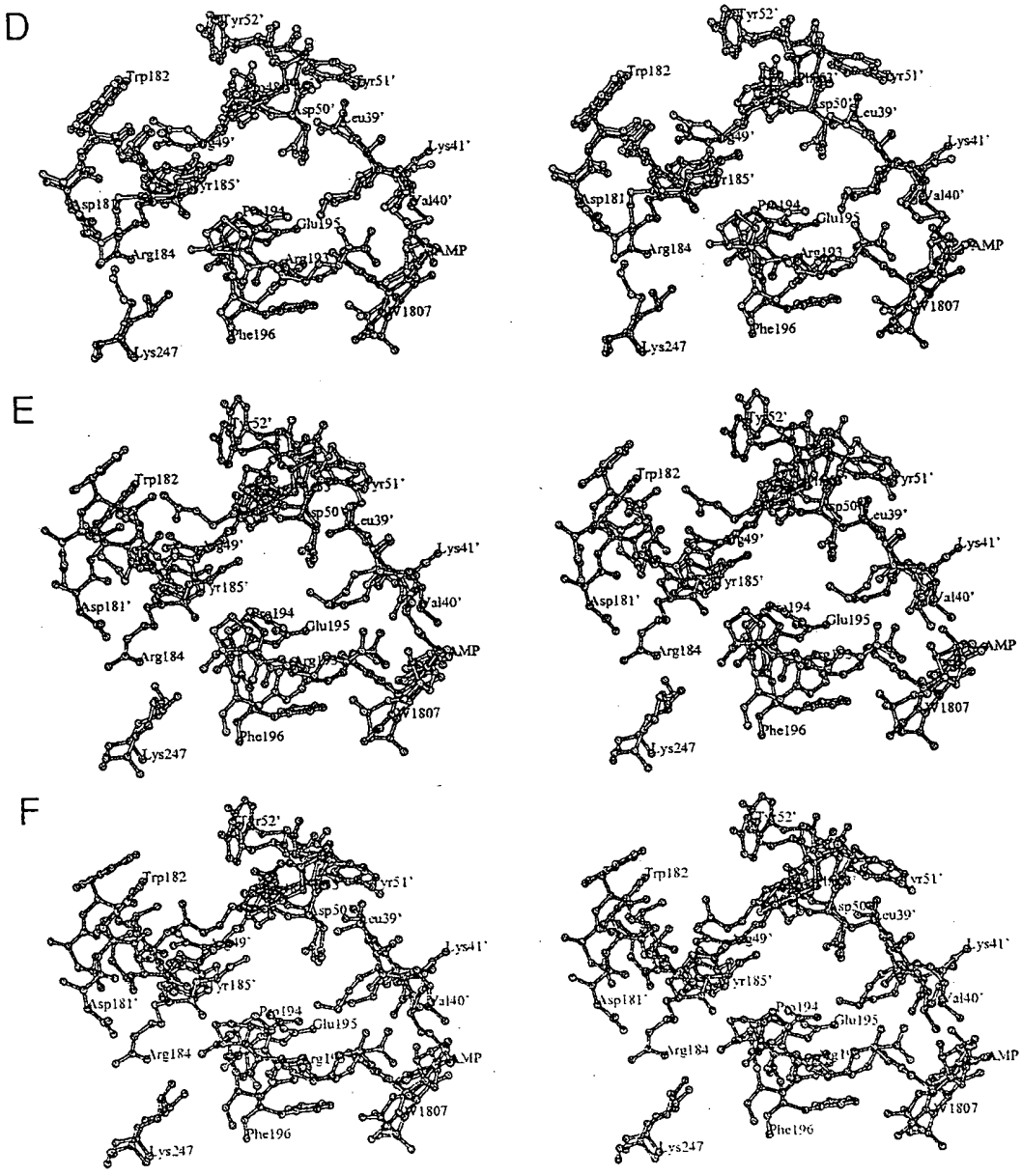

Fig. 8. *Continued.*

refined by the conventional positional and restrained individual *B*-factor refinement protocol in X-PLOR 3.8 to give a final *R*-factor value of 17.9% (R_{free} = 23.0%). The final structure contained residues 5–250, 261–313, 325–838, and 807 water molecules. The average *B*-factors for main-chain, side-chain atoms, PLP, Glc, Ser14-*P*, a glycerol molecule (assigned at a later stage), and water molecules were 22.1, 24.8, 19.9, 22.7, 29.9, 32.9, and 34.4 Å^2, respectively. Residues where *B*-factor values exceed 60 Å^2 include 16–21 (overall atomic ⟨*B*⟩ factors 64.6 Å^2). The average *B*-factors (main-chain atoms) for residues 5–26 were 43.5 Å^2 or 36.6 Å^2 (if residues 16–21 were excluded). The same region (16–21) is also poorly ordered in the structure of the room temperature enzyme complex (Sprang et al., 1988). The program PROCHECK (Laskowski et al., 1993) was used to examine the stereochemistry of the model. The Ramachandran plot shows 89.7% of residues in the most favored regions, 9.6% of residues in the additional allowed regions, 0.5% of residues (four residues) in the generously allowed regions, and 0.1% of residues (one residue, Asp6) in the disallowed regions.

Refinement of the GPa-Glc-W1807 complex was performed with XPLOR (version 3.8) (Brünger, 1996). All data between 13.0 and 2.1 Å were included with no sigma cut-offs. The starting structure was the 2.0 Å refined structure of the T-state GPa-Glc complex (see above). The Fourier maps calculated with SIGMAA (Read, 1986) weighted ($F_o - F_c$) and ($2F_o - F_c$) coefficients indicated binding of Glc at the catalytic site and W1807 at the allosteric site. The maps also indicated that the side chain of Arg309 had shifted into the allosteric site to contact the carboxylate oxygens O2 and O3 of the inhibitor. A model of W1807 (Zographos et al., 1997) was fitted to the density at the allosteric site and Glc at the catalytic site. Water molecules in the GPa-Glc-W1807 complex were examined, and those displaced by the ligand were removed. The final model was subjected to conventional positional and restrained individual *B*-factor refinement to give a final *R*-factor value of 18.9% (R_{free} = 26.3%). The final structure contained residues 5–250, 260–314, 325–835, and 784 water molecules. The average *B*-factors were 28.0 (main-chain atoms), 29.7 (side-chain atoms), 24.2 (PLP), 26.5 (W1807), (25.9) Glc, 100.0 (Ser14-*P*), 33.3 (glycerol), and 35.7 Å^2 (water molecules), respectively. Residues where overall ⟨*B*⟩-factors values (given in parentheses) exceed 60 Å^2 include 5–26 (94.4 Å^2), 209–211 (66.2 Å^2), 554 (62.4 Å^2), and 831–835 (70.9 Å^2). The Ramachandran plot shows 90.4% of residues in the most favored regions, 8.9% of residues in the additional allowed regions, 0.5% of residues in the generously allowed regions, and only Asp6 (0.1% of residues) in the disallowed regions.

Refinement of the GPb-W1807-glycerol complex, by using the structure of the GPb-Glc complex (PDB accession 2GPB) as a starting model for X-PLOR (version 3.1) (Brünger, 1992), to a crystallographic *R*-value of 19.8% (R_{free} = 28.7%) for data between 8.0 and 2.3 Å, was described previously (Zographos et al., 1997). Further crystallographic refinement of GPb-W1807-glycerol complex performed using the version 3.8 of the X-PLOR by applying solvent mask correction and including all reflections between 30 and 2.3 Å was recently described (Tsitsanou et al., 1999).

The structures were analyzed with the graphics program O (Jones et al., 1991). Hydrogen bonds were assigned if the distance between the electronegative atoms was less than 3.3 Å and if both angles between these atoms and the preceding atoms were greater than 90°. Van der Waals interactions were assigned for nonhydrogen atoms separated by less than 4°. The protein structures were compared using LSQKAB (CCP4, 1994).

Coordinate sets for comparison were: room temperature T-state GPa-Glc complex (Sprang et al., 1988), T-state GPa-Glc-AMP complex (Sprang et al., 1987), T-state 100K GPb (Gregoriou et al., 1998) (PDB code 2GPN), T-state 100K GPb-W1807 complex (Zographos et al., 1997) (PDB code 2AMV), room temperature R-state GPa (Barford et al., 1991) (PDB code 1GPA), room temperature R-state GPb-AMP complex (Barford et al., 1991) (PDB code 7GPB), and room temperature PLPP-GPb-AMP (Sprang et al., 1991) (PDB code 1PYG). Coordinates for T-state 100K GPa-Glc and GPa-Glc-W1807 complexes have been deposited with the Protein Data Bank, Brookhaven National Laboratory, Upton, New York (PDB codes 2GPA and 3AMV, respectively).

Acknowledgments

This work was supported by a Wellcome Trust Biomedical Research Collaboration Grant to NGO (with Prof. L.N. Johnson) and the EU contract ERB FMGE CT95 0022 (ELETTRA, Trieste, Italy) through minor grant to NGO. We are grateful to Prof. L.N. Johnson for critical reading, Prof. R.J. Fletterick and Prof. S.R. Sprang for providing the atomic coordinates for RT T-state GPa-Glc complex and T-state GPa-Glc-AMP complex structures, and Dr. M. Gregoriou for help in the production of figures.

References

Barford D, Hu SH, Johnson LN. 1991. Structural mechanism for glycogen phosphorylase control by phosphorylation and AMP. *J Mol Biol 218*:233–260.

Barford D, Johnson LN. 1989. The allosteric transition of glycogen phosphorylase. *Nature 340*:609–616.

Bollen M, Stalmans W. 1992. The structure, role, and regulation of type-1 protein phosphatases. *Crit Rev Biochem Mol Biol 27*:227–281.

Brünger AT. 1992. *X-PLOR version 3.1. A system for X-ray crystallography and NMR*. New Haven and London: Yale University Press.

Brünger AT. 1996. *X-PLOR version 3.8*. New Haven, CT: Department of Molecular Biophysics and Biochemistry, Yale University.

Cohen P. 1973. The subunit structure of rabbit-skeletal-muscle phosphorylase kinase, and the molecular basis of its activation reactions. *Eur J Biochem 34*:1–14.

CCP4 (Collaborative Computational Project, Number 4). 1994. The CCP4 Suite: Programs for protein crystallography. *Acta Crystallogr D 50*:760–763.

Fischer EH, Krebs EG. 1962. Muscle phosphorylase *b*. *Methods Enzymol 5*:369–373.

Fletterick RJ, Madsen NB. 1980. The structures and related functions of phosphorylase *a*. *Ann Rev Biochem 49*:31–61.

Fletterick RJ, Sygusch J, Murray N, Madsen NB, Johnson LN. 1976. Low-resolution structure of the glycogen phosphorylase *a* monomer and comparison with phosphorylase *b*. *J Mol Biol 103*:1–13.

Gregoriou M, Noble MEM, Watson KA, Garman EF, Krulle TM, Fuente C. Fleet GWJ, Oikonomakos NG, Johnson LN. 1998. The structure of a glycogen phosphorylase spirohydantoin complex at 1.8 Å resolution and 100 K: The role of the water structure and its contribution to binding. *Protein Sci 7*:915–927.

Helmreich EJM, Cori CF. 1964. The role of adenylic acid in the activity of phosphorylase. *Proc Natl Acad Sci USA 51*:131–138.

Johnson LN. 1992. Glycogen phosphorylase: Control by phosphorylation and allosteric effectors. *FASEB J 6*:2274–2282.

Johnson LN, Hajdu J, Acharya KR, Stuart DI, McLaughlin PJ, Oikonomakos NG, Barford D. 1989. Glycogen phosphorylase *b*. In: Herve G, ed. *Allosteric enzymes*. Boca Raton, FL: CRC Press. pp 81–127.

Johnson LN, Martin JL, Acharya KR, Barford D, Oikonomakos NG. 1993. The refined crystal structure of the glycogen phosphorylase-glucose 6-phosphate complex. *J Mol Biol 232*:253–267.

Jones TA, Zou JY, Cowan SW, Kjeldgaard M. 1991. Improved methods for the building of protein models in electron density maps and the location of errors in these models. *Acta Crystallogr A47*:110–119.

Kastenschmidt LL, Kastenschmidt J, Helmreich EJM. 1968. Subunit interactions and their relationship to the allosteric properties of rabbit skeletal muscle phosphorylase *b*. *Biochemistry 7*:3590–3608.

Kasvinsky PJ, Shechosky S, Fletterick RJ. 1978. Synergistic regulation of phosphorylase *a* by glucose and caffeine. *J Biol Chem 253*:9102–9106.

Laskowski RA, MacArthur MW, Moss DS, Thorton JM. 1993. PROCHECK: A program to check the stereochemical quality of protein structures. *J Appl Cryst 26*:283–291.

Madsen NB. 1986. Glycogen phosphorylase. In: Boyer PD, Krebs EG, eds. *The enzymes*, 3rd ed., vol 17. New York: Academic Press. pp 366–394.

Martin JL, Veluraja K, Johnson LN, Fleet GWJ, Ramsden NG, Bruce I, Oikonomakos NG, Papageorgiou AC, Leonidas DD, Tsitoura HS. 1991. Glucose analogue inhibitors of glycogen phosphorylase: The design of potential drugs for diabetes. *Biochemistry 30*:10101–10116.

Martin WH, Hoover DJ, Armento SJ, Stock IA, McPherson RK, Danley DE, Stevenson RW, Barrett EJ, Treadway JL. 1998. Discovery of a human glycogen phosphorylase inhibitor that lowers blood glucose in vivo. *Proc Natl Acad Sci USA 95*:1776–1781.

Melpidou AE, Oikonomakos NG. 1983. Effect of glucose-6-P on the catalytic and structural properties of glycogen phosphorylase. *FEBS Lett 154*:105–110.

Monod J, Changeux JP, Jacob F. 1965. On the nature of allosteric transitions: A plausible model. *J Mol Biol 12*:88–118.

Oikonomakos NG, Acharya KR, Johnson LN. 1992. Rabbit muscle glycogen phosphorylase *b*: Structural basis of activation and catalysis. In: Harding JJ, Crabbe MJC, eds. *Post-translational modification of proteins*. Boca Raton, FL: CRC Press. pp 81–151.

Oikonomakos NG, Kontou M, Zographos SE, Watson KA, Johnson LN, Bichard CJF, Fleet GWJ, Acharya KR. 1995a. N-acetyl-β-D-glucopyranosylamine: A potent T state inhibitor of glycogen phosphorylase. A comparison with α-D-glucose. *Protein Sci 4*:2469–2477.

Oikonomakos NG, Zographos SE, Johnson LN, Papageorgiou AC, Acharya KR. 1995b. The binding of 2-deoxy-glucose-6-phosphate to glycogen phosphorylase *b*: Kinetic and crystallographic studies. *J Mol Biol 254*:900–917.

Otwinowski Z. 1993. DENZO. Data collection and processing, DL/SC1/R34. Daresbury, Warrington, UK: SERC Laboratory.

Owen DJ, Papageorgiou AC, Garman EF, Noble MEM, Johnson LN. 1995. Expression, purification and crystallization of phosphorylase kinase catalytic domain. *J Mol Biol 246*:374–381.

Read RJ. 1986. Improved Fourier coefficients for maps using phases from partial structures with errors. *Acta Crystallogr A 42*:140–149.

Segel IH. 1975. *Enzyme kinetics*. New York: Wiley Interscience. pp 465–504.

Sprang SR, Acharya KR, Goldsmith EJ, Stuart DI, Varvill K, Fletterick RJ, Madsen NB, Johnson LN. 1988. Structural changes in glycogen phosphorylase induced by phosphorylation. *Nature 336*:215–221.

Sprang SR, Goldsmith E, Fletterick R. 1987. Structure of the nucleotide activation switch in glycogen phosphorylase *a*. *Science 237*:1012–1019.

Sprang SR, Goldsmith EJ, Fletterick RJ, Withers SG, Madsen NB. 1982. Catalytic site of glycogen phosphorylase: Structure of the T state and specificity for α-D-glucose. *Biochemistry 21*:5364–5371.

Sprang SR, Withers SG, Goldsmith EJ, Fletterick RJ, Madsen NB. 1991. Structural basis for activation of glycogen phosphorylase *b* by adenosine monophosphate. *Science 254*:1367–1371.

Street IP, Armstrong CR, Withers SG. 1986. Hydrogen bonding and specificity. Fluorodeoxy sugars as probes of hydrogen bonding in the glycogen phosphorylase-glucose complex. *Biochemistry 25*:6021–6027.

Tsitsanou KE, Oikonomakos NG, Zographos SE, Skamnaki VT, Gregoriou M, Watson KA, Johnson LN, Fleet GWJ. 1999. The effect of most commonly used cryoprotectants on glycogen phosphorylase activity and structure. *Protein Sci 8*:741–749.

Zographos SE, Oikonomakos NG, Tsitsanou KE, Leonidas DD, Chrysina ED, Skamnaki VT, Bischoff H, Goldmann S, Schram M, Watson KA, Johnson LN. 1997. The structure of glycogen phosphorylase *b* with an alkyldihydropyridine-dicarboxylic acid compound, a novel and potent inhibitor. *Structure 5*:1413–1425.

This Page is Inserted by IFW Indexing and Scanning Operations and is not part of the Official Record

BEST AVAILABLE IMAGES

Defective images within this document are accurate representations of the original documents submitted by the applicant.

Defects in the images include but are not limited to the items checked:

- ☐ BLACK BORDERS
- ☐ IMAGE CUT OFF AT TOP, BOTTOM OR SIDES
- ☒ FADED TEXT OR DRAWING
- ☒ BLURRED OR ILLEGIBLE TEXT OR DRAWING
- ☐ SKEWED/SLANTED IMAGES
- ☐ COLOR OR BLACK AND WHITE PHOTOGRAPHS
- ☐ GRAY SCALE DOCUMENTS
- ☐ LINES OR MARKS ON ORIGINAL DOCUMENT
- ☐ REFERENCE(S) OR EXHIBIT(S) SUBMITTED ARE POOR QUALITY
- ☐ OTHER: _____

IMAGES ARE BEST AVAILABLE COPY.
As rescanning these documents will not correct the image problems checked, please do not report these problems to the IFW Image Problem Mailbox.

THIS PAGE BLANK (USPTO)